Generation and evolution of mode-locked noise-like square-wave pulses in a large-anomalous-dispersion Er-doped ring fiber laser

Jun Liu,[1] Yu Chen,[1] Pinghua Tang,[2] Changwen Xu,[1] Chujun Zhao,[1,2,*] Han Zhang,[1] and Shuangchun Wen[2]

[1]SZU-NUS Collaborative Innovation Center for Optoelectronic Science & Technology, Key Laboratory of Optoelectronic Devices and Systems of Ministry of Education and Guangdong Province, College of Optoelectronic Engineering, Shenzhen University, Shenzhen 518060, China
[2]Laboratory for Micro-/Nano- Optoelectronic Devices of Ministry of Education, School of Physics and Electronics, Hunan University, Changsha 410082, China
[*]chujunzhao@gmail.com

Abstract: In a passively mode-locked Erbium-doped fiber laser with large anomalous-dispersion, we experimentally demonstrate the formation of noise-like square-wave pulse, which shows quite different features from conventional dissipative soliton resonance (DSR). The corresponding temporal and spectral characteristics of a variety of operation states, including Q-switched mode-locking, continuous-wave mode-locking and Raman-induced noise-like pulse near the lasing threshold, are also investigated. Stable noise-like square-wave mode-locked pulses can be obtained at a fundamental repetition frequency of 195 kHz, with pulse packet duration tunable from 15 ns to 306 ns and per-pulse energy up to 200 nJ. By reducing the linear cavity loss, stable higher-order harmonic mode-locking had also been observed, with pulse duration ranging from 37 ns at the 21st order harmonic wave to 320 ns at the fundamental order. After propagating along a piece of long telecom fiber, the generated square-wave pulses do not show any obvious change, indicating that the generated noise-like square-wave pulse can be considered as high-energy pulse packet for some promising applications. These experimental results should shed some light on the further understanding of the mechanism and characteristics of noise-like square-wave pulses.

OCIS codes: (140.0140) Lasers and laser optics; (140.3510) Lasers, fiber; (140.4050) Mode-locked lasers.

References and links

1. A. M. Kaplan, G. P. Agrawal, and D. N. Maywar, "Optical square-wave clock generation based on an all-optical flip-flop," IEEE Photon. Technol. Lett. **22**(7), 489–491 (2010).
2. X. Peng, B. Jordens, A. Hooper, B. W. Baird, W. Ren, L. Xu, and L. Sun, "Generation of programmable temporal pulse shape and applications in micromachining," Proc. SPIE **7193**, 719324 (2009).
3. R. Evans, S. Camacho-López, F. G. Pérez-Gutiérrez, and G. Aguilar, "Pump-probe imaging of nanosecond laser-induced bubbles in agar gel," Opt. Express **16**(10), 7481–7492 (2008).
4. X. Liu, "Coexistence of strong and weak pulses in a fiber laser with largely anomalous dispersion," Opt. Express **19**(7), 5874–5887 (2011).
5. X. Zhang, C. Gu, G. Chen, B. Sun, L. Xu, A. Wang, and H. Ming, "Square-wave pulse with ultra-wide tuning range in a passively mode-locked fiber laser," Opt. Lett. **37**(8), 1334–1336 (2012).
6. V. J. Matsas, T. P. Newson, and M. N. Zervas, "Self-starting passively mode-locked fiber ring laser exploiting nonlinear polarization switching," Opt. Commun. **92**(1-3), 61–66 (1992).
7. M. A. Putnam, M. L. Dennis, I. N. Duling Iii, C. G. Askins, and E. J. Friebele, "Broadband square-pulse operation of a passively mode-locked fiber laser for fiber Bragg grating interrogation," Opt. Lett. **23**(2), 138–140 (1998).
8. L. M. Zhao, D. Y. Tang, T. H. Cheng, and C. Lu, "Nanosecond square pulse generation in fiber lasers with normal dispersion," Opt. Commun. **272**(2), 431–434 (2007).
9. X. Wu, D. Y. Tang, H. Zhang, and L. M. Zhao, "Dissipative soliton resonance in an all-normal-dispersion erbium-doped fiber laser," Opt. Express **17**(7), 5580–5584 (2009).

#230599 - $15.00 USD Received 11 Dec 2014; revised 5 Feb 2015; accepted 16 Feb 2015; published 2 Mar 2015

10. L. Mei, G. Chen, L. Xu, X. Zhang, C. Gu, B. Sun, and A. Wang, "Width and amplitude tunable square-wave pulse in dual-pump passively mode-locked fiber laser," Opt. Lett. **39**(11), 3235–3237 (2014).
11. H. Lin, C. Guo, S. Ruan, and J. Yang, "Dissipative soliton resonance in an all-normal-dispersion Yb-doped figure-eight fibre laser with tunable output," Laser Phys. Lett. **11**(8), 085102 (2014).
12. S. K. Wang, Q. Y. Ning, A. P. Luo, Z. B. Lin, Z. C. Luo, and W. C. Xu, "Dissipative soliton resonance in a passively mode-locked figure-eight fiber laser," Opt. Express **21**(2), 2402–2407 (2013).
13. Z. C. Luo, W. J. Cao, Z. B. Lin, Z. R. Cai, A. P. Luo, and W. C. Xu, "Pulse dynamics of dissipative soliton resonance with large duration-tuning range in a fiber ring laser," Opt. Lett. **37**(22), 4777–4779 (2012).
14. L. Duan, X. Liu, D. Mao, L. Wang, and G. Wang, "Experimental observation of dissipative soliton resonance in an anomalous-dispersion fiber laser," Opt. Express **20**(1), 265–270 (2012).
15. W. Chang, A. Ankiewicz, J. M. Soto-Crespo, and N. Akhmediev, "Dissipative soliton resonances," Phys. Rev. A **78**(2), 023830 (2008).
16. W. Chang, J. M. Soto-Crespo, A. Ankiewicz, and N. Akhmediev, "Dissipative soliton resonances in the anomalous dispersion regime," Phys. Rev. A **79**(3), 033840 (2009).
17. X. Li, X. Liu, X. Hu, L. Wang, H. Lu, Y. Wang, and W. Zhao, "Long-cavity passively mode-locked fiber ring laser with high-energy rectangular-shape pulses in anomalous dispersion regime," Opt. Lett. **35**(19), 3249–3251 (2010).
18. H. Liu, X. Zheng, N. Zhao, Q. Ning, M. Liu, Z. Luo, A. Luo, and W. Xu, "Generation of multiwavelength noise-like square-pulses in a fiber laser," IEEE Photon. Technol. Lett. **26**(19), 1990–1993 (2014).
19. X. W. Zheng, Z. C. Luo, H. Liu, N. Zhao, Q. Y. Ning, M. Liu, X. H. Feng, X. B. Xing, A. P. Luo, and W. C. Xu, "High-energy noise-like rectangular pulse in a passively mode-locked figure-eight fiber laser," Appl. Phys. Express **7**(4), 042701 (2014).
20. S. Keren, E. Brand, Y. Levi, B. Levit, and M. Horowitz, "Data storage in optical fibers and reconstruction by use of low-coherence spectral interferometry," Opt. Lett. **27**(2), 125–127 (2002).
21. A. Zaytsev, C. H. Lin, Y. J. You, C. C. Chung, C. L. Wang, and C. L. Pan, "Supercontinuum generation by noise-like pulses transmitted through normally dispersive standard single-mode fibers," Opt. Express **21**(13), 16056–16062 (2013).
22. S. M. J. Kelly, "Characteristic sideband instability of periodically amplified average soliton," Electron. Lett. **28**(8), 806 (1992).
23. T. North and M. Rochette, "Raman-induced noiselike pulses in a highly nonlinear and dispersive all-fiber ring laser," Opt. Lett. **38**(6), 890–892 (2013).
24. Y. Jeong, L. A. Vazquez-Zuniga, S. Lee, and Y. Kwon, "On the formation of noise-like pulses in fiber ring cavity configurations," Opt. Fiber Technol. **20**(6), 575–592 (2014).

1. Introduction

High energy square-wave pulses in nanosecond time scales have attracted considerable attention due to their potential applications, including all-optical square-wave clocks, laser micromachining, range finding, and optical sensing [1–5]. Passively mode-locked fiber lasers are an ideal candidate to directly produce such kind of pulses, offering a compact and cost-effective laser cavity associated with an excellent beam quality and flexible pulse duration. This typical operation state of square-wave pulse exists in a fiber laser passively mode-locked by either nonlinear polarization rotation (NPR) technique [6–9] or figure of eight configuration [10–12]. The square-wave pulse generation was primarily attributed to the nonlinear polarization switching inside the laser cavity [6] or the dissipative soliton resonance (DSR) [12]. Besides, the generation of square-wave pulse is theoretically and experimentally demonstrated to be independent of the cavity dispersion [9, 12–16]. In the DSR region, the square-wave pulses could increase their width indefinitely while keeping their amplitude constant. High energy square-wave profile dissipative solitons in an all-normal-dispersion fiber laser were obtained in [9], with the pulse duration tunable from 0.6 ns to 18.5 ns. Li et al. demonstrated a square-wave pulse from 33.3 to 155.4 ns with maximum output pulse energy of 79.5 nJ in the anomalous dispersion regime by varying the pump power [17]. It is worth noting that these square-wave pulses were reported to have no internal fine structures within the square profile packet, and therefore they maintain the pulse-to-pulse coherence. However, this coherent square-wave pulse generation requires extremely rigorous cavity parameter selections and is usually difficult to obtain.

Another similar noise-like square-wave pulse demonstrated more recently [18, 19] exhibits nearly the same characteristic as that formed through DSR except that they lack or partially lack a temporal coherence because of the bunch of short pulses with stochastic duration, peak power and pulse number located in the square packet. These noise-like square-wave pulses with great duration tuning flexibility can be easily obtained in a cavity with high

#230599 - $15.00 USD Received 11 Dec 2014; revised 5 Feb 2015; accepted 16 Feb 2015; published 2 Mar 2015

nonlinearity. In addition, their energy can also be increased to a large value and thus can be potentially applied in many important areas, such as low spectral coherence interferometry, micromachining, and supercontinuum (SC) generation [20, 21]. In particular, the detailed nature of generation and evolution of noise-like pulse can provide a better understanding of the fundamental physics for pulse transmission in nonlinear fiber-optic media. However, there are few reports on the pulse evolution of the noise-like square-wave pulses up to now.

In this paper, we investigate the noise-like square-wave pulse generation and evolution in a passively mode-locked Er-doped fiber laser based on the NPR technique. Stable noise-like square-wave mode-locked pulses at the fundamental repetition frequency of 195 kHz are obtained with maximum intra-cavity single pulse energy of 200 nJ. The square-wave pulse width can be tuned from 15 ns to 306 ns by varying the pump power with fixed alignment of the polarization controllers (PCs). By further increasing the pump power, stable noise-like square-wave pulses in the cavity break up into two well-distinguished pulses, leading to a second-order harmonic square-wave mode-locking regime, which is distinctly different from the traditional DSR effect. By employing another laser cavity with lower loss, stable higher-order harmonic mode-locking of noise-like square-wave pulses can be obtained by finely adjusting the cavity parameters. At the same launched pump power of 805 mW, square-wave pulses with various repetition rates from the fundamental one (195 kHz) to the 21st order harmonic (4.1 MHz) had been obtained by adjusting the orientation of PCs, with pulse duration ranging from 320 ns to 37 ns, respectively.

2. Experiment and results

2.1 The experimental setup

The experimental schematic diagram of the mode-locked fiber laser is shown in Fig. 1. The ring laser cavity consists of a piece of 2.5 m Er-doped gain fiber (EDF, Liekki, Er110), two sections of 500 m standard single-mode telecom fiber (SMF, G652 and G653), two sets of PCs, a polarization-dependent isolator (PD-ISO), a fused 30% or 2% output coupler (OC), a 1480 nm high power single-mode Raman pump source with maximum output power of up to 10 W (KEOPSYS), and two 1480/1550 nm wavelength-division-multiplexed (WDM) couplers. The PD-ISO and two PCs, together of which operate as an artificial saturable absorber, are responsible for the self-started stable mode locking of the fiber laser. The EDF and the G652 SMF have a group velocity dispersion (GVD) of −9 ps/nm/km and 17 ps/nm/km at 1550 nm, respectively, resulting in a large net cavity dispersion of ~-12 ps^2.

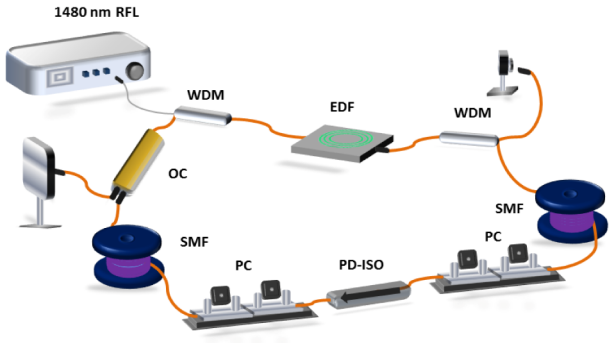

Fig. 1. Experimental schematic of the mode-locked fiber laser for square-wave pulse generation. WDM: wavelength division multiplexer; SMF: single mode fiber; PC: polarization controller; PD-ISO: polarization-dependent isolator; OC: output coupler.

The output power from the Raman pump source was directly coupled into the EDF through the 1480/1550 nm WDM coupler. Another similar WDM coupler was employed to couple the unabsorbed pump power out of the cavity to eliminate the influence of the residual pump power.

#230599 - $15.00 USD Received 11 Dec 2014; revised 5 Feb 2015; accepted 16 Feb 2015; published 2 Mar 2015

An optical spectrum analyzer (Ando, AQ-6317B) and a real time oscilloscope with a bandwidth of 4 GHz (Agilent Technol., DSO9404A) together with a 5 GHz photoelectric detector (Thorlabs, SIR5) were simultaneously used to monitor the output spectrum and the pulse train. Moreover, the radio frequency (RF) spectra were measured by a RF-spectrum analyzer (Agilent, N9322C). Fine structures of the pulse profile were measured with a commercial autocorrelator (FR-103-XL).

2.2 Different pulsed regimes of the mode-locked fiber laser

The output coupling ratio of the laser cavity was first set to be 30%. The laser can operate in four different stable or quasi-stable lasing regimes around the threshold through the alignment of PCs to vary the net cavity birefringence. These operating regimes include the conventional soliton generation, Q-switched and continuous-wave mode-locking of square-wave pulses, and Raman-induced noise-like pulses. At the launched pump power of ~40 mW, the conventional soliton mode-locking regime can be initiated. The corresponding temporal trace and spectrum are illustrated in Fig. 2(a) and Fig. 3, respectively.

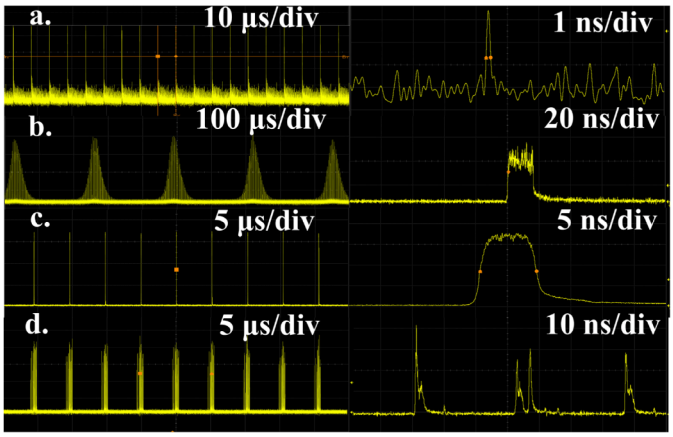

Fig. 2. Temporal profiles for a variety of pulsed operating regimes at the lasing threshold. a: conventional solitons; b: Q-switched mode-locking square-wave pulses; c: continuous-wave mode-locking square-wave pulses; d: Raman-induced noise-like pulses.

The output spectrum shows clear sidebands and the autocorrelation trace of the conventional solitons was measured to be a coherent $sech^2$ profile without pedestal [22], as shown in Fig. 4. The Q-switched and continuous-wave mode-locking of square-wave pulses can also be observed, as shown in Fig. 2(b) and Fig. 2(c), respectively. An obvious feature in both operating regimes is that the single pulse exhibits a square-shape profile on oscilloscope. Both of the corresponding autocorrelation traces in Fig. 4 consist of a narrow spike riding on a broad shoulder that extended over the entire scanning time window. The pedestal duration was too long to be traced properly within the scanning time window of the available autocorrelator, therefore exhibiting a square-shape profile. Both autocorrelation traces indicate that the square-wave pulses at the Q-switched and continuous-wave mode-locking possess random fine structures, well-known as the noise-like pulses. In addition, it is worth noting that the output spectrum (see Fig. 3) and the autocorrelation trace for the Q-switched mode-locking regime are randomly distributed in a particularly modulated envelope in contrast to the relatively smooth profiles at the continuous-wave mode-locking regime, which confirms that the intermediate and transitional state of Q-switched mode-locking is unstable before the emergence of continuous-wave mode-locking. The formation of Q-switched mode-locking is attributed to the birefringence-induced loss modulation at a low level of pump power. The output spectrum of the continuous-wave mode-locking regime exhibits a much smoother and broader profile without any sideband or other fine internal structure than that of the conventional soliton operating regime, which is the other typical characteristic of the

#230599 - $15.00 USD Received 11 Dec 2014; revised 5 Feb 2015; accepted 16 Feb 2015; published 2 Mar 2015

noise-like pulses. In addition, the Raman-induced noise-like pulse with a ~2 μs long burst of nanosecond envelope comprising picosecond-scale oscillations had also been observed, as shown in Fig. 2(d). Similar experimental results have been recently reported in [23]. The corresponding spectrum was largely broadened through the stimulated Raman scattering effect resulting from the high nonlinearity in the cavity.

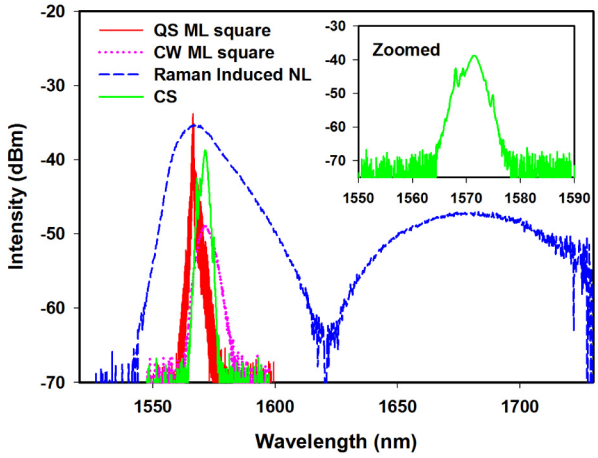

Fig. 3. Corresponding output spectra for the various operating regimes at the lasing threshold, including the conventional mode-locked solitons (CS), Q-switched mode-locking square-wave pulses (QS ML square), continuous-wave mode-locking square-wave pulses (CW ML square) and Raman-induced noise-like pulses (Raman induced NL). Inset: zoomed spectrum of CS operating regime.

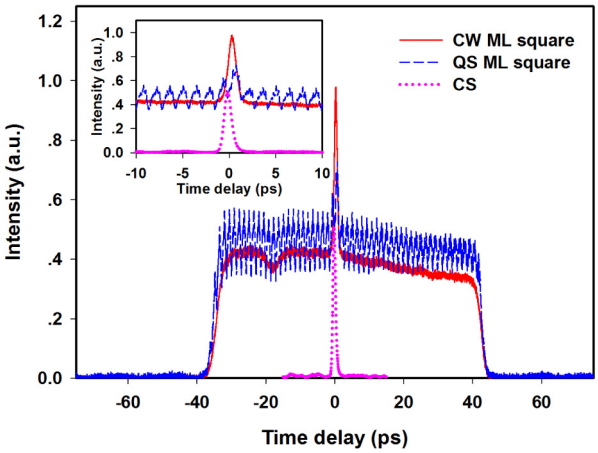

Fig. 4. Corresponding autocorrelation traces for the various operating regimes at the lasing threshold, including the conventional mode-locked solitons (CS), Q-switched mode-locking square-wave pulses (QS ML square), and continuous-wave mode-locking square-wave pulses (CW ML square). Inset: corresponding autocorrelation traces under a small scanning range.

2.3 Noise-like square-wave mode-locked pulses

Self-starting continuous-wave noise-like square-wave mode-locked pulses at the fundamental repetition rate were obtained with a lasing threshold of ~43 mW. By fixing the PCs, the square-wave pulse broadened with the pump strength while the corresponding pulse amplitude remained constant. The evolution of pulse duration and average power on the

#230599 - $15.00 USD Received 11 Dec 2014; revised 5 Feb 2015; accepted 16 Feb 2015; published 2 Mar 2015

launched pump power for the particular arrangement of the PCs is shown in Fig. 5. It can be seen that both the pulse width and average power increase almost linearly with the pump power up to 1085 mW. A further increase of the pump power will render the system unstable and ultimately evolves into the second-order harmonic square-wave mode-locking. This situation is distinctly different from the DSR effect, where the pulse energy can be accumulated infinitely to a large value without pulse breaking. Figure 6 depicts the temporal evolution of the noise-like square-wave pulses at different pump powers, where the measured pulse width broadened from 15 ns to 306 ns with the pump power increasing from 43 mW to 1085 mW. The fundamental pulse repetition rate is 195 kHz, corresponding to the total cavity length, and the signal-to-noise ratio (SNR) is about 53 dB, as shown in Fig. 7. The evolution of the lasing output spectrum at different pump powers is depicted in Fig. 8. The spectral intensity increases slightly with the pump power while the 3 dB bandwidths of the spectra remain nearly invariable. By keeping the pump power constant and slightly adjusting the polarization controller under the stable mode-locking operating regime, the central wavelength shifted in a small range of around ± 3 nm, and the spectrum shows no clearly resolved peaks.

The stable self-starting noise-like square-wave pulses, in nanosecond time scale, were generated based on the nonlinear polarization switching inside the laser cavity [6]. The switching power depends on the gain and loss in the laser cavity, which ultimately determines the peak power of square-wave pulses. Once the intra-cavity pulse power reaches the switching power, the peak power will be clamped. Due to the intrinsic soliton formation and peak power clamping effect in large-anomalous dispersion operating regime, pulse breaking effect occurs and fine internal structures were found to exist inside the square-wave pulses. The square-wave pulse broadened with the increasing pump power until the gain in the cavity got saturated. The corresponding saturation pump power in our experiment is 1085 mW. The whole lasing system will grow unstable after a further increase of the pump power, and ultimately evolves into the second-order harmonic square-wave mode-locking.

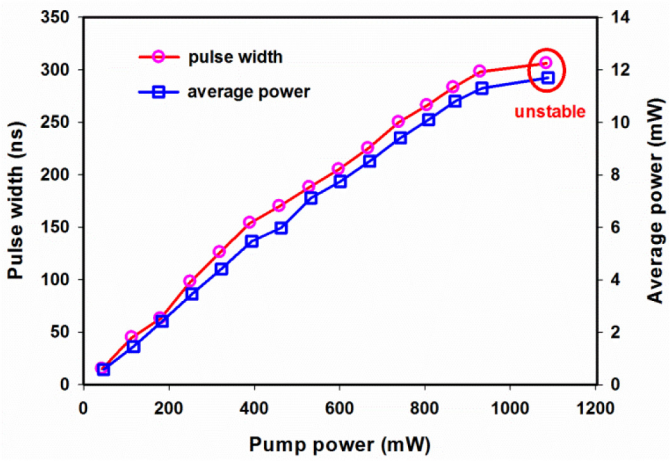

Fig. 5. Measured square-wave pulse width and average output power as a function of the pump power.

#230599 - $15.00 USD Received 11 Dec 2014; revised 5 Feb 2015; accepted 16 Feb 2015; published 2 Mar 2015

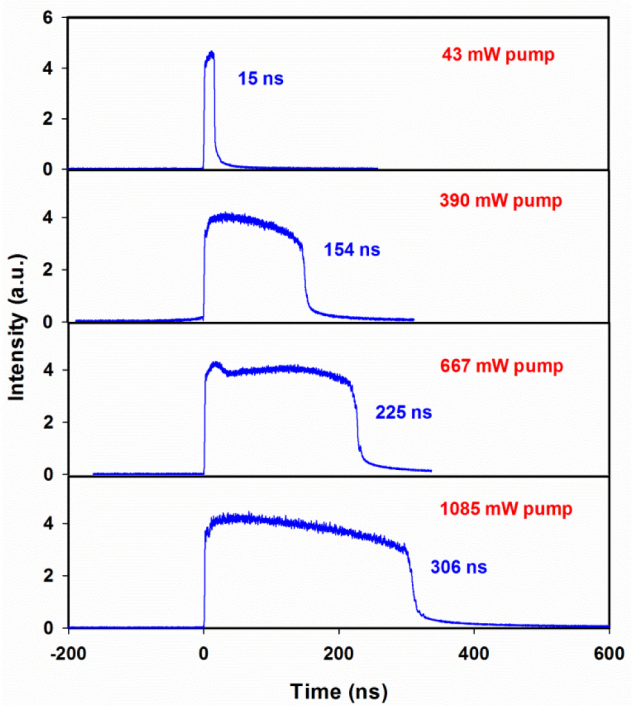

Fig. 6. Evolution of the single square-wave pulse under different pump powers.

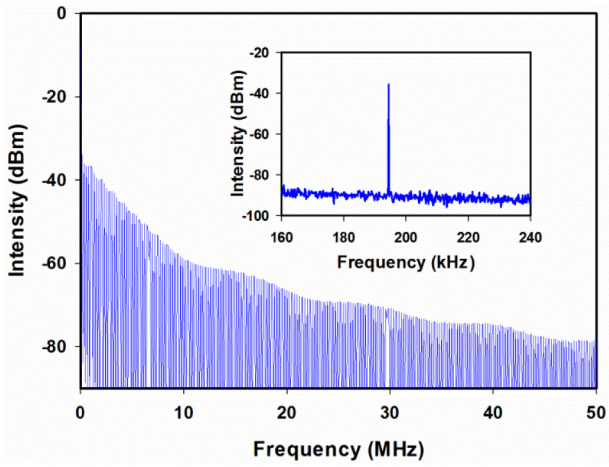

Fig. 7. RF spectrum of the mode-locked noise-like square-wave pulses.

To further investigate the noise-like square-wave pulse evolution, particularly on the generation of higher-order harmonic mode-locking of square-wave pulses, we reduce the cavity loss by substituting a 2% output coupler for the 30% one and thus the saturation pump power is lowered correspondingly. Stable continuous-wave mode-locked square-wave pulses at the fundamental frequency were obtained with the lasing threshold of ~30 mW. The square-wave pulses stretched until the output power get saturated at the pump power of 805 mW. Similarly, the second-order harmonic mode-locking occurred by further increasing the pump power. Due to the much reduced cavity loss resulting from a smaller output coupling ratio, the

#230599 - $15.00 USD Received 11 Dec 2014; revised 5 Feb 2015; accepted 16 Feb 2015; published 2 Mar 2015

intra-cavity pulses experienced a larger nonlinearity and the polarization switching threshold is lower.

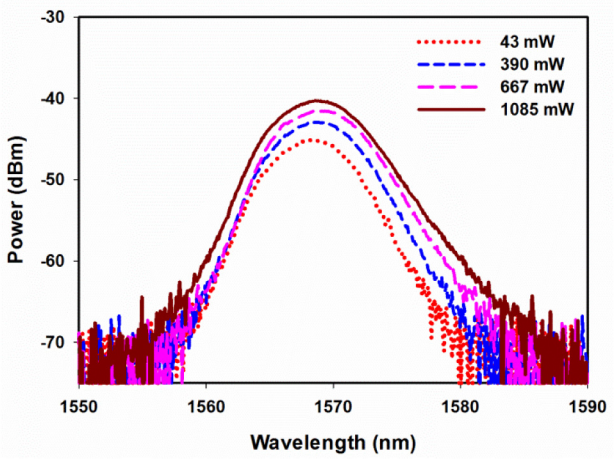

Fig. 8. Measured output spectra at different pump powers.

With launched pump power fixed at 805 mW, the square-wave pulse packet can split into two or more, subsequently leading to a peak power reduction, by proper adjustment of the PCs. This makes the laser system operating in a higher-order harmonic square-wave mode-locking regime. In our experiment, up to 21st order harmonic mode-locked noise-like square-wave pulses at the repetition rate of 4.1 MHz was achieved through the PCs' alignment to vary the net cavity birefringence. The typical pulse trains of different order harmonic mode-locking are shown in Fig. 9.

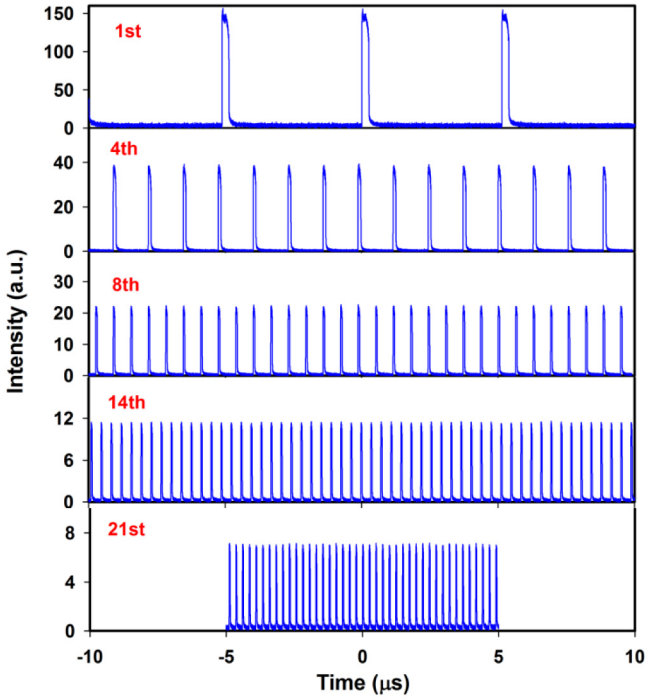

Fig. 9. Harmonic mode-locked square-wave pulse trains of different orders achieved at the same pump power of 805 mW.

#230599 - $15.00 USD Received 11 Dec 2014; revised 5 Feb 2015; accepted 16 Feb 2015; published 2 Mar 2015

The square-wave pulse duration ranged from 37 ns at the 21st order harmonic wave to 320 ns at the fundamental wave. The autocorrelation trace of the harmonic mode-locked square-wave pulses was also characterized as a coherent peak located on a broad pedestal, indicating that the harmonic mode-locked square-wave pulses were a similar type as the fundamental mode-locked ones, known as the noise-like pulses. The RF spectrum of the 21st order harmonic mode-locked square-wave pulses is shown in Fig. 10. The side-mode suppression ratio is measured to be about 36 dB, which demonstrates a stable harmonic mode-locking. The mutual evolution for higher-order harmonic mode-locking by aligning the PCs indicates that that for a specific set of cavity parameters the peak-clamping effect could also be imposed on noise-like square-wave pulses, similar to the mechanism occurring in the multi-soliton formation [3, 24].

The propagation characteristics of the noise-like square-wave pulses obtained were evaluated by launching it into a 10.6 km standard single mode telecom fiber. We observed no difference on the square-wave pulse profile and spectrum before and after the propagation except the pulse width increasing from 62.7 ns to 63.5 ns at the launched pump power of 180 mW, indicating that the so called noise-like square-wave pulse can be considered as a high-energy pulse packet and thus be capable of being employed in many applications.

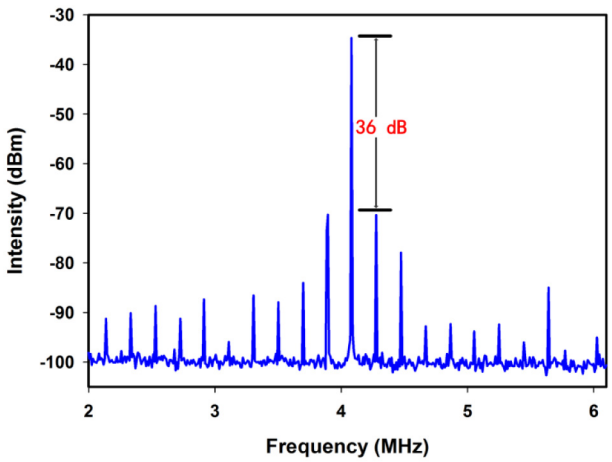

Fig. 10. RF spectrum of the 21st order harmonic mode-locked square-wave pulses.

3. Conclusion

In conclusion, the generation and evolution of noise-like square-wave pulses from a mode-locked Er-doped fiber laser operating in a large-anomalous-dispersion regime were experimentally demonstrated. This type of noise-like square-wave pulse distinctly differs from the conventional DSR effect. There exist several random internal short pulses within the noise-like square-wave profile. Stable noise-like square-wave mode-locked pulses were achieved at a fundamental repetition frequency of 195 kHz, with pulse duration tunable from 15 ns to 306 ns by increasing the pump power, and the maximum intra-cavity single pulse energy reaches up to 200 nJ. This fundamental square-wave mode-locked pulse can evolve into a stable higher-order harmonic mode-locking of noise-like square-wave pulses by adjusting the cavity parameters, which is attributed to the peak-clamping effect imposed on the noise-like square-wave pulses. Undistorted propagation properties in a long traditional telecom fiber demonstrate that the noise-like square-wave pulses have a potential use in many applications as a high-energy pulse packet. The experimental results should possibly facilitate further research on the mechanism and characteristics of nanosecond square-wave pulses.

#230599 - $15.00 USD Received 11 Dec 2014; revised 5 Feb 2015; accepted 16 Feb 2015; published 2 Mar 2015

Acknowledgments

This work is partially supported by the National 973 Program of China (Grant No. 2012CB315701), the National Natural Science Fund Foundation of China (Grant Nos. 61435010 and 61475102) and Natural Science Foundation of SZU (Grant No. 201453).

#230599 - $15.00 USD Received 11 Dec 2014; revised 5 Feb 2015; accepted 16 Feb 2015; published 2 Mar 2015